Discrete Mechanics and Variational Integrators: Applications to Celestial Mechanics

AME 599 – Advance Dynamics (Spring 2007), Professor Eva Kanso

Try Lam*

This paper investigates the use of a variational integrator for problems in celestial mechanics, specifically, the planar circular restricted three-body problem and the simplified *N*-body solar system problem (Sun, Jupiter, Saturn, and Uranus). The variational integrator used is derived using the trapezoidal rule or the Störmer-Verlet rule. Comparisons are made between the 2nd order variational integrator to that of the 4th order Runge-Kutta.

Introduction

In this paper we investigate the application of a variational integrator, which uses the discrete Euler-Lagrange equation, to selected problems in celestial mechanics. A key fact about variational integrators and the reason why it is investigated here is that variational integrators are symplectic. In general, symplectic integrators are numerical schemes to solve Hamilton's equation which preserves the same two-form (symplectic manifold) $\Omega = dp \wedge dq$ on state space as the true system. In other words, the manifold or the set of all possible configuration of the system is conserved or the vector field preserves a certain differential form, i.e., one remains on the manifold of the system. The class of integrators which does are called symplectic integrators. A consequence of symplectic flow is that areas in phase space are conserved.

Exact solutions to Hamilton's equation is that the Hamilton is constant along all solutions, i.e., $\dot{H} = 0$, then an integrator which discretize the equations should also preserve this. Other integrators which arbitrary discretize the Hamilton's equations may not keep *H* constant along solutions and sometimes may introduce drifts from the true solutions [1-4].

It is noted that although symplectic integrators conserved the Hamiltonian of the system it is usually a quantity which is perturbed from that of the true system. It is also well known that being symplectic does not guarantee accuracy of the solution [2]. One should measure the capability of variational integrators on its reproducibility of families of solutions and accurate prediction of statistical results. This approach respects, by construction, the conserved quantities in the mechanical system, conserved total momentum. Variational integrators also have the property of conserving momentum maps. A remark showed in [3] is that fixed step size numerical integrators can only be symplectic and momentum preserving or energy and momentum preserving. This paper will focus on the later former.

* Graduate student, University of Southern California, Los Angeles. Try.Lam@jpl.nasa.gov

Due to the symplectic nature of variational integrators it is widely used for long-term evolution of chaotic system as in molecular dynamics or celestial mechanics. This paper will derive and implement a variational integrator for the planar circular restricted three-body problem (PCR3BP) and the simplified 4-body solar system model, containing only the Sun, Jupiter, Saturn, and Uranus.

Variational integrators differ from other symplectic integrators because it is derived by using the Lagrangian instead of the Hamiltonian to create an integrator based on discrete variational principles. Details on the formulation are in Wendlandt and Marsden [4] and West [5-6]. This method approximate the action integral with a quadrature rule to give the discrete Lagrangian, and then applies a discrete variational principle to get the discrete Euler-Lagrange equations. Previous approaches in developing symplectic integrators used generating functions and Hamilton-Jacobi equations [7].

The next section will briefly review the continuous Lagrange mechanics and the derivation of the Euler-Lagrange equations. An analogues derivation of the discrete Euler-Lagrange equations will be then be made, where we will consider the trapezoidal or Störmer-Verlet method as our quadrature rule, which is commonly used for molecular dynamics problem, and show how to write it as a variational integrator. The derivation of Störmer-Verlet method as a variational integrator is in Wendlandt and Marsden [4], and briefly described in this paper. Discussion on the symplectic nature of the integrator will then be made. This will be followed by two examples (1) the PCR3BP and (2) the simplified 4-body Solar System.

Lagrange Mechanics

In this section a brief review of the derivation of the Euler-Lagrange equations. Considering N particles in the $\mathbb{E}^3$ space, which can be represented as q_i for all N particles in the configuration space Q where $i = 1,\ldots,3N$.

The most general form of the Lagrangian function L is define as a function of the position and velocities given by

$$L(q_i, \dot{q}_i) = T(\dot{q}_i) - V(q_i) \tag{1}$$

where $T(\dot{q}_i) = \frac{1}{2}\sum_i m_i (\dot{q}_i)^2$ is the kinetic energy and $V(q_i)$ is the potential energy. For simplicity, vector notations will be used to obtain the Lagrangian of the form

$$L(q, \dot{q}) = \frac{1}{2}\dot{q}^T M \dot{q} - V(q) \tag{2}$$

where M is a symmetric positive-definite matrix. Considering all smooth paths $q(t)$ in Q with fixed end points at time t_0 and t_1, then to each path a number called the action S is assigned, and is given by

$$S[q(t)] = \int_{t_0}^{t_1} L(q, \dot{q}) dt \,. \tag{3}$$

Hamilton's Principle states that of all the possible that can be taken, the actual physical path taken is a stationary point of *S*, i.e., $\delta S = 0$. In other words, to compute the variations of the action while holding the endpoints of the curve $q(t)$ fixed. This gives

$$\delta S = \delta \int_{t_0}^{t_1} L(q, \dot{q}) dt = \int_{t_0}^{t_1} \delta L(q, \dot{q}) dt = \int_{t_0}^{t_1} \left(\frac{\partial L}{\partial q} \delta q + \frac{\partial L}{\partial \dot{q}} \delta \dot{q} \right) dt = 0$$

Integrating the last term by parts and setting $\delta q(t_0) = \delta q(t_1) = 0$, we have

$$\delta S = \int_{t_0}^{t_1} \left(\frac{\partial L}{\partial q} - \frac{d}{dt} \frac{\partial L}{\partial \dot{q}} \right) \delta q = 0$$

Requiring that the variations of the action be zero for all δq implies that the integrand of the equation above must be zero for each time t, which then gives rise to the Lagrange's equations or *Euler-Lagrange equations*

$$\frac{\partial L}{\partial q} - \frac{d}{dt} \frac{\partial L}{\partial \dot{q}} = 0 \,. \tag{4}$$

For the Lagrangian given by Eq. (2) the Euler-Lagrange equation becomes Newton's equation,

$$M\ddot{q} = -\nabla V(q) \,. \tag{5}$$

Discrete Lagrange Mechanics

We now show the discrete variational mechanics analog to the above derivation. Considering the system with configuration manifold *Q* and, thus, a velocity phase space (tangent bundle) *TQ*, the Lagrangian is then a map *L*: *TQ* → R. In discrete mechanics we replace *TQ* with *Q* x *Q*, and, thus, take two nearby points as the discrete analogue of a velocity vector. Consider two positions q_k and q_{k+1} and a time Δt rather than taking a position q and $\dot{q}$. Now consider a discrete Lagrangian approximating the action integral along the segment between q_k and q_{k+1} by quadrature rule of interpolating functions:

$$L_d(q_k, q_{k+1}) \approx \int_{t_k}^{t_{k+1}} L(q, \dot{q}) \, dt \tag{6}$$

An example of such method is using the rectangular rule ($q = q_k$) and the approximation $\dot{q} \approx (q_{k+1} - q_k)/\Delta t$. Assuming the Lagrangian in Eq. (2), then the discrete Lagrangian is then of the form

$$L_d(q_k, q_{k+1}) = \left[\frac{1}{2} \left(\frac{q_{k+1} - q_k}{\Delta t} \right)^T M \left(\frac{q_{k+1} - q_k}{\Delta t} \right) - V(q_k) \right] \Delta t \,. \tag{7}$$

Another example is the midpoint rule, where $q = (q_{k+1} + q_k)/2$ and $\dot{q} \approx (q_{k+1} - q_k)/\Delta t$. The discrete Lagrangian for the midpoint rule is then of the form

$$\begin{aligned} L_d(q_k, q_{k+1}) &= L\left(\frac{q_{k+1} + q_k}{2}, \frac{q_{k+1} - q_k}{\Delta t} \right) \Delta t \\ &= \left[\frac{1}{2} \left(\frac{q_{k+1} - q_k}{\Delta t} \right)^T M \left(\frac{q_{k+1} - q_k}{\Delta t} \right) - V\left(\frac{q_{k+1} + q_k}{2} \right) \right] \Delta t \end{aligned} \,. \tag{8}$$

Applying the trapezoidal rule (also known as the Verlet or Störmer rule) the discrete Lagrangian for the midpoint rule is then of the form

$$\begin{aligned} L_d(q_k, q_{k+1}) &= \frac{1}{2} \left[L\left(q_k, \frac{q_{k+1} - q_k}{\Delta t} \right) + L\left(q_{k+1}, \frac{q_{k+1} - q_k}{\Delta t} \right) \right] \Delta t \\ &= \frac{1}{2} \left[\left(\frac{q_{k+1} - q_k}{\Delta t} \right)^T M \left(\frac{q_{k+1} - q_k}{\Delta t} \right) + V(q_{k+1}) - V(q_k) \right] \Delta t \end{aligned} \tag{9}$$

This method was originally formulated for molecular dynamics problem [2]. Other rules such as the Newmark method (widely used in structural dynamics codes) exits, but for demonstration purposes we will focus on the trapezoidal rule. Another reason for selected the trapezoidal rule over the midpoint or rectangular rule is that it the method is explicit, which we will show later.

Now consider a discrete curve made up of points q_k for $k = 0, ..., N$ and calculating the discrete action along this sequence by summing the discrete Lagrangian,

$$S_d[q_k] = \sum_{k=0}^{N-1} L_d(q_k, q_{k+1}) \tag{10}$$

Analogous to the continuous derivation we compute the variations of the action sum with the boundary points q_0 and q_N being held fixed. This gives

$$\delta S_d[q_k] = \delta \sum_{k=0}^{N-1} L_d(q_k, q_{k+1}) = \sum_{k=0}^{N-1} \left[\frac{\partial L_d(q_k, q_{k+1})}{\partial q_k} \delta q_k + \frac{\partial L_d(q_k, q_{k+1})}{\partial q_{k+1}} \delta q_{k+1} \right] = 0 \quad (11)$$

Rearranging the summation and setting $\delta q_0 = \delta q_N = 0$, we have

$$\delta S_d[q_k] = \sum_{k=0}^{N-1} \left[\left(\frac{\partial L_d(q_k, q_{k+1})}{\partial q_k} + \frac{\partial L_d(q_{k-1}, q_k)}{\partial q_{k+1}} \right) \delta q_k \right] = 0 ,$$

and hence we have the *discrete Euler-Lagrange equations*

$$\frac{\partial L_d(q_k, q_{k+1})}{\partial q_k} + \frac{\partial L_d(q_{k-1}, q_k)}{\partial q_{k+1}} = 0 . \quad (12)$$

For the Lagrangian given by Eq. (2) the discrete Euler-Lagrange equation becomes a discretization of Newton's equation,

$$M \left(\frac{q_{k+1} - 2q_k + q_{k-1}}{(\Delta t)^2} \right) = -\nabla V(q_k) . \quad (13)$$

The power of this method is clear from Eqs. (12) and (13). Given a set of initial conditions (q_0, q_1), which should approximate $q_0 \approx q(t_0)$ and $q_1 \approx q(t_0 + \Delta t)$, then the discrete Euler-Lagrange equations define a recursive rule for calculating the entire sequence of q_k for $k = 0,..., N$, that we can think of as an integrator for the continuous system.

Variational Integrators

As stated above discrete Lagrangian mechanics provide a method to map states for mechanics systems for an entire discrete trajectory, i.e., it acts as an integrator. These special integrators which use the discrete Euler-Lagrange equation are known as *variational integrators*.

For many mechanical systems we specify initial conditions by stating an initial position and velocity. Eq. (12) or (13) requires one specify the initial two position q_0 and q_1. Thus we must re-write the Eq. (12) in position-velocity (or momentum) form. In this paper we will state without proof that the momentum at time step *k* to be

$$p_k = \frac{\partial L_d(q_{k-1}, q_k)}{\partial q_{k+1}} = -\frac{\partial L_d(q_k, q_{k+1})}{\partial q_k} . \quad (14)$$

Detail and proof of this momentum form can be found in Section 1.5 of Marsden and West (2001), or one can view this derivation as a result of the Hamiltonian view of discrete mechanics. Using this definition we have

$$p_k = -\frac{\partial L_d(q_k, q_{k+1})}{\partial q_k} \tag{15a}$$

$$p_{k+1} = \frac{\partial L_d(q_k, q_{k+1})}{\partial q_{k+1}} \tag{15b}$$

Now given a set of position-momentum initial conditions (q_0, p_0) we can solve the implicit equation (15a) to find q_1, and then use the explicit equation (15b) to give p_1. Thus, equation (15) provides a map for calculating the entire sequence of q_k and p_k for $k = 0,..., N$.

For the trapezoidal method and for the discrete Lagrangian of the form equation (9), equations (15) becomes

$$p_k = M\left(\frac{q_{k+1} - q_k}{\Delta t}\right) + \frac{1}{2}\nabla V(q_k)\Delta t \tag{16a}$$

$$p_{k+1} = M\left(\frac{q_{k+1} - q_k}{\Delta t}\right) - \frac{1}{2}\nabla V(q_{k+1})\Delta t \tag{16b}$$

Rearranging (16a) we get (17a) and subtracting (16a) from (16b) and solving for q_{k+1} we obtain (17b)

$$q_{k+1} = q_k + (\Delta t)M^{-1}p_k - \frac{1}{2}(\Delta t)^2 M^{-1}(\nabla V(q_k)) \tag{17a}$$

$$p_{k+1} = p_k - \frac{1}{2}(\Delta t)(\nabla V(q_{k+1}) + \nabla V(q_k)) \tag{17b}$$

Equations (17) provides an explicit method mapping the entire sequence of q_k and p_k.

Symplectic Nature of Variational Integrators

Independent of the choice of the discrete Lagrangian variational integrators are symplectic and momentum conserving. Momentum preserving means that when the discrete system has a symmetry, then there is a discrete Noether theorem that gives a quantity that is exactly conserved at the discrete level [8]. Consider a one-parameter group of curve $q^\alpha(t)$, with $q^0(t) = q(t)$, which as the property that $L(q^\alpha, \dot{q}^\alpha) = L(q, \dot{q})$ for all α. If the Lagrangian is invariant under S then we have a symmetry. If the Lagrangian is invariant then the action integral is also invariant, so have

$$0 = \frac{\partial}{\partial \alpha} S(q)\Big|_{\alpha=0} = \frac{\partial}{\partial \alpha} \int_{t_0}^{t_1} L(q,\dot{q}) dt \Big|_{\alpha=0}$$
$$= \frac{\partial}{\partial \dot{q}} L(q(t_1),\dot{q}(t_1)) \frac{\partial q^{\alpha}(t_1)}{\partial \alpha}\Big|_{\alpha=0} - \frac{\partial}{\partial \dot{q}} L(q(t_0),\dot{q}(t_0)) \frac{\partial q^{\alpha}(t_0)}{\partial \alpha}\Big|_{\alpha=0}$$

The equations above shows that the final and initial momenta in the direction of $\partial q^{\alpha}(t)/\partial \alpha\big|_{\alpha=0}$. This is Noether's theorem [9]. Similarly for the discrete system we have discrete Noether's theorem

$$\frac{\partial L_d(q_{N-1},q_N)}{\partial q_{k+1}} \frac{\partial q_k^{\alpha}}{\partial \alpha}\Big|_{\alpha=0} = \frac{\partial L_d(q_0,q_1)}{\partial q_k} \frac{\partial q_k^{\alpha}}{\partial \alpha}\Big|_{\alpha=0}$$

for a one-parameter group of discrete time curve q_k^{α} for $k = 0,...,N$ with $q_k^0 = q_k$, and such that the discrete Lagrangian is invariant for all α and k.

In addition to the conservation of energy and momenta, Lagrangian systems are also symplectic for example Liouville's theorem, for more reference see [9] and [10]. Accordingly, a discrete analogous for symplectic form for the continuous Lagrangian system exist as a consequence of the variational structure for the continuous and discrete system.

Example 1: Planar Circular Restricted Three Body Problem (PCR3BP)

A common dynamical model in astrodynamics with high sensitivity is the three body problem [11]. A simplification to the general three body problem is the planar circular restricted three body problem, where a mass m_2 orbits mass m_1 in a circular obit and a third negligible mass m_3 orbits without restriction around both in the m_1 and m_2 orbit plane. Normalizing the problem such that $\omega^2(m_1 m_2)^3 = G(m_1+m_2) = 1$ and $\mu = m_2/(m_1+m_2)$ where G is the universal gravitation constant and ω is the rotation rate of m_2 about m_1, we have

$$\ddot{x} - 2\dot{y} - x = -(1-\mu)\frac{x-x_1}{r_1^3} - \mu\frac{x-x_2}{r_2^3} = -\frac{\partial V}{\partial x}$$
$$\ddot{y} + 2\dot{x} + y = -(1-\mu)\frac{y}{r_1^3} - \mu\frac{y}{r_2^3} = -\frac{\partial V}{\partial y} \qquad (18)$$

where $V = -(1-\mu)/r_1 - \mu/r_2$ and $\mu = m_2/(m_1+m_2)$. The equations are derived in the rotating frame centered at the center of mass, where m_1 and m_2 are fixed on the x-axis. Due to the normalization the positions are such that $x_1 = 1-\mu$ and $x_2 = \mu$, thus $r_1^2 = (x+\mu)^2 + y^2$ and $r_2^2 = (x-1+\mu)^2 + y^2$.

The Lagrangian is expressed as

$$L = \frac{1}{2}\left[(\dot{x} - y)^2 + (\dot{y} + x)^2\right] + \frac{1-\mu}{r_1} + \frac{\mu}{r_2} \tag{19}$$

From the first part of Eq. (9), which is

$$L_d(q_k, q_{k+1}) = \frac{1}{2}\left[L\left(q_k, \frac{q_{k+1} - q_k}{\Delta t} \right) + L\left(q_{k+1}, \frac{q_{k+1} - q_k}{\Delta t} \right) \right] \Delta t \tag{9a}$$

Then the discrete Lagrangian is

$$\begin{aligned} L_d = \frac{1}{2}\Bigg[\frac{1}{2}\Bigg[\left(\frac{x_{k+1} - x_k}{\Delta t} - y_k \right)^2 + \left(\frac{y_{k+1} - y_k}{\Delta t} + x_k \right)^2 \Bigg] + \frac{1-\mu}{r_{k,1}} + \frac{\mu}{r_{k,2}} \\ + \frac{1}{2}\Bigg[\left(\frac{x_{k+1} - x_k}{\Delta t} - y_{k+1} \right)^2 + \left(\frac{y_{k+1} - y_k}{\Delta t} + x_{k+1} \right)^2 \Bigg] + \frac{1-\mu}{r_{k+1,1}} + \frac{\mu}{r_{k+1,2}} \Bigg] \Delta t \end{aligned} \tag{20}$$

where $r_{k,1} = \sqrt{(x_k + \mu)^2 + y_k^2}$ and $r_{k,2} = \sqrt{(x_k - 1 + \mu)^2 + y_k^2}$.

Using Eq. (15) to solve for p_k and p_{k+1}, we get the following

$$p_{x,k} = -\frac{\partial L_d}{\partial x_k} = \frac{x_{k+1} - x_k}{\Delta t} - y_{k+1} - \frac{1}{2}(\Delta t)x_k + \frac{\Delta t}{2}\frac{(1-\mu)(x_k + \mu)}{r_{k,1}^3} + \frac{\Delta t}{2}\frac{\mu(x_k - 1 + \mu)}{r_{k,2}^3} \tag{21a}$$

$$p_{x,k+1} = \frac{\partial L_d}{\partial x_{k+1}} = \frac{x_{k+1} - x_k}{\Delta t} - y_k + \frac{1}{2}(\Delta t)x_{k+1} - \frac{\Delta t}{2}\frac{(1-\mu)(x_{k+1} + \mu)}{r_{k+1,1}^3} - \frac{\Delta t}{2}\frac{\mu(x_{k+1} - 1 + \mu)}{r_{k+1,2}^3} \tag{21b}$$

$$p_{y,k} = -\frac{\partial L_d}{\partial y_k} = \frac{y_{k+1} - y_k}{\Delta t} + x_{k+1} - \frac{1}{2}(\Delta t)y_k + \frac{\Delta t}{2}\frac{(1-\mu)y_k}{r_{k,1}^3} + \frac{\Delta t}{2}\frac{\mu y_k}{r_{k,2}^3} \tag{21c}$$

$$p_{y,k+1} = \frac{\partial L_d}{\partial y_{k+1}} = \frac{y_{k+1} - y_k}{\Delta t} + x_k + \frac{1}{2}(\Delta t)y_{k+1} - \frac{\Delta t}{2}\frac{(1-\mu)y_{k+1}}{r_{k+1,1}^3} - \frac{\Delta t}{2}\frac{\mu y_{k+1}}{r_{k+1,2}^3} \tag{21d}$$

Now, rearranging (21a) and solving for x_{k+1}, we get

$$x_{k+1} = x_k\left(1 + \frac{1}{2}(\Delta t)^2\right) + (\Delta t)y_{k+1} + (\Delta t)p_{x,k} - \frac{(\Delta t)^2}{2}\left[\frac{(1-\mu)(x_k + \mu)}{r_{k,1}^3} + \frac{\mu(x_k - 1 + \mu)}{r_{k,2}^3}\right] \tag{22}$$

Note that the equation above is dependent on y_{k+1}. To solve (22) explicitly, we must rearranging (21c) and solving for y_{k+1}, we get

$$y_{k+1} = y_k\left(1+\frac{1}{2}(\Delta t)^2\right) - (\Delta t)x_{k+1} + (\Delta t)p_{y,k} - \frac{(\Delta t)^2 y_k}{2}\left[\frac{(1-\mu)}{r_{k,1}^3} + \frac{\mu}{r_{k,2}^3}\right] \tag{23}$$

Substituting (23) into (22) and re-solving for x_{k+1}, we have

$$\begin{aligned} x_{k+1} = \frac{1}{1+(\Delta t)^2}\Bigg[&\left(1+\frac{1}{2}(\Delta t)^2\right)\left(x_k + (\Delta t)y_k\right) + \Delta t\left(p_{x,k} + (\Delta t)p_{y,k}\right) \\ &- \frac{(\Delta t)^3 y_k}{2}\left[\frac{(1-\mu)}{r_{k,1}^3} + \frac{\mu}{r_{k,2}^3}\right] - \frac{(\Delta t)^2}{2}\left[\frac{(1-\mu)(x_k+\mu)}{r_{k,1}^3} + \frac{\mu(x_k-1+\mu)}{r_{k,2}^3}\right]\Bigg] \end{aligned} \tag{24}$$

Subtracting (21a) from (21b) and (21c) from (21d), the corresponding momentum along the x and y-axis, respectively are

$$\begin{aligned} p_{x,k+1} = p_{x,k} &+ \frac{\Delta t}{2}\left(x_{k+1}+x_k\right) + \left(y_{k+1}-y_k\right) - \frac{(\Delta t)(1-\mu)}{2}\left[\frac{(x_k+\mu)}{r_{k,1}^3} + \frac{(x_{k+1}+\mu)}{r_{k+1,1}^3}\right] \\ &- \frac{(\Delta t)\mu}{2}\left[\frac{(x_k-1+\mu)}{r_{k,2}^3} + \frac{(x_{k+1}-1+\mu)}{r_{k+1,2}^3}\right] \end{aligned} \tag{25}$$

$$\begin{aligned} p_{y,k+1} = p_{y,k} &- \left(x_{k+1}-x_k\right) + \frac{\Delta t}{2}\left(y_{k+1}+y_k\right) \\ &- \frac{(\Delta t)(1-\mu)}{2}\left[\frac{y_k}{r_{k,1}^3} + \frac{y_{k+1}}{r_{k+1,1}^3}\right] - \frac{(\Delta t)\mu}{2}\left[\frac{y_k}{r_{k,2}^3} + \frac{y_{k+1}}{r_{k+1,2}^3}\right] \end{aligned} \tag{26}$$

Given a set of initial conditions $\left[x_0, y_0, p_{x,0}, p_{y,0}\right]$ Eqs. (23-26) allows us to map the states from step k to k+1 explicitly. We note that for the PCR3BP $p_x = \partial L/\partial \dot{x} = \dot{x} - y$ and $p_y = \partial L/\partial \dot{y} = \dot{y} + x$, and thus $\dot{x} = p_x + y$ and $\dot{y} = p_y - x$. This provides us with a method to relate velocities to momentum.

For the CR3BP there is a constant of motion known as the Jacobi constant, which is the only integral of motion for the system, and for the planar case it is defined as

$$J_C = \left(x^2 + y^2\right) + 2\left(\frac{1-\mu}{r_1} + \frac{\mu}{r_2}\right) - \left(\dot{x}^2 + \dot{y}^2\right). \tag{27}$$

As an exercise, we will take the Sun-Earth system as an example, μ = 3.04036e-006. Taking the initial conditions X_0 = [0.6, 0, 0, -2], we map or propagate the trajectory for 300 time units (normalized or equivalently 17,439.4 years for this example). As stated above the Jacobi constant for the CR3BP is the only integral of motion, and thus the only conserved quantity we can use to compare the variational integrator developed above to non-variational integrators. In this example we will compare the variational integrator with that of ODE45 and ODE4 (or RK4)

in Matlab, variable step size 4^{th}-5^{th} order Runge-Kutta and the fixed step size 4^{th} order Runge-Kutta, respectively. The trajectory propagated using ODE45 is considered our "true" trajectory. For ODE45 we selected a tolerance of 1E-10 for the relative and absolute tolerances. For the RK4 and the variational integrator we selected a step size of 0.0001.

We expect the Jacobi constant to oscillate about a constant for the variational integrator, and to see a slight drift for the other cases. Figure 1 shows the trajectory using the initial conditions above for the first 5 normalized time units (or 291 years for the system). Note that visually, one cannot tell any differences between the trajectories for the three integrators. Figure 2(a) and 3(a) shows the change in the Jacobi constant for all three integrators. Note the expected cyclic nature of the variational integrator, and the drift for the ODE45 trajectory. Surprising the case integrated using RK4 remains the most constant. Figure 2(b) and 3(b) shows that the state differences between the variational integrator and ODE45 integrator are larger than those of the RK4 and ODE45. The integration times for the runs were 101.078 secs for the variational integrators, 296.813 secs for the RK4 integrator, and 248.766 secs for the ODE45.

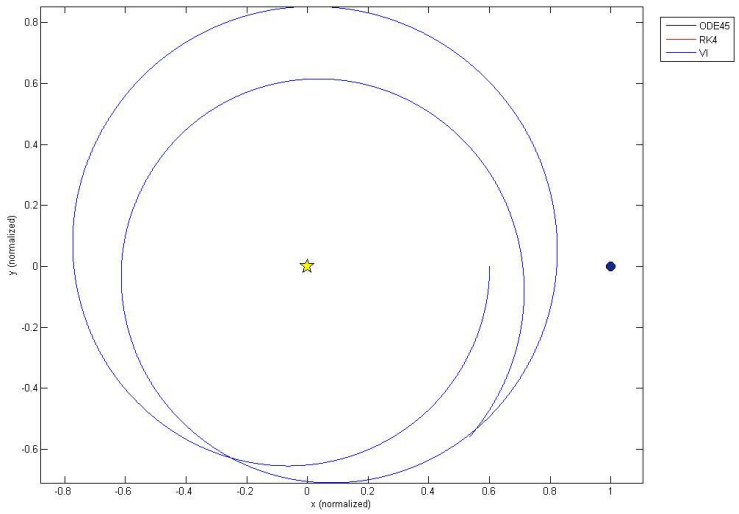

Figure 1. Trajectories propagated for 5 normalized time unit for the Sun-Earth system (μ = 3.04036e-006) for the following initial conditions, X_0 = [0.6, 0, 0, -2], using ODE45, RK4, and the variational integrator. ☆ is the location of the Sun, O is the location of the Earth.

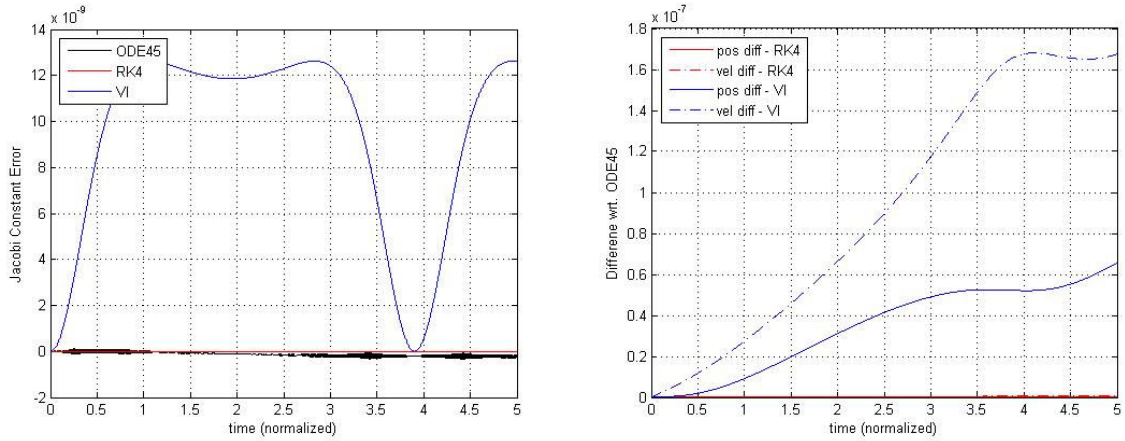

Figure 2. Integrated for 5 time units. (a) The error in the Jacobi constant, and (b) the differences in position and velocity for the RK4 and variational integrator when compared to the ODE45 trajectory for the Sun-Earth system (μ = 3.04036e-006) for the following initial conditions, X_0 = [0.6, 0, 0, -2].

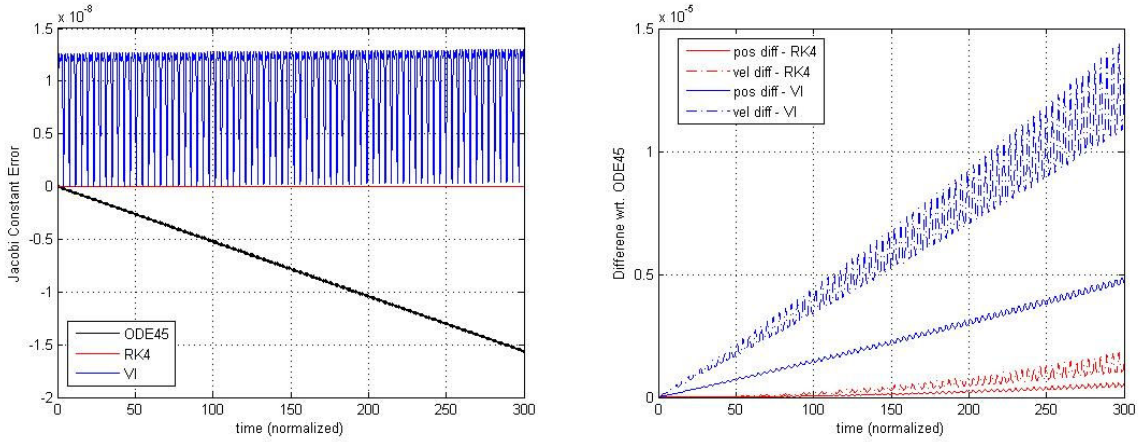

Figure 2. Integrated for 300 time units. (a) The error in the Jacobi constant, and (b) the differences in position and velocity for the RK4 and variational integrator when compared to the ODE45 trajectory for the Sun-Earth system (μ = 3.04036e-006) for the following initial conditions, X_0 = [0.6, 0, 0, -2].

To get an ideal of the behavior in a more global perspective Poincaré (or suface of sections) map were created for the *y=0* phase plot, $\dot{x}$ versus x. The initial conditions used to generate the map were for x = -1.2 to 1.2 with step size of 0.1 (excluding points near singularities, i.e., x = 0 and 1) and for $\dot{y}$ = -0.1 to -2 of step size 0.1. Each trajectory was integrated for 100 time units. The range of run times was 9-11 seconds for the variational integrator, 22-33 seconds for the RK4, and 22-200 seconds for the ODE45. The upper values for the ODE45 cases were due to the propagations near singularities, i.e., near one of the primary bodies. Figure 3 shows the Poincaré map for the ODE45 integrations. Note that one can see the existence of librating (quasi-periodic) orbits and near periodic orbits, and those in the "chaotic sea". Figure 4 is the Poincaré map for the variational integrator, note the similarity of map to Figure 3. The only notable difference is the lack of data points near x = 0 in Figure 4.

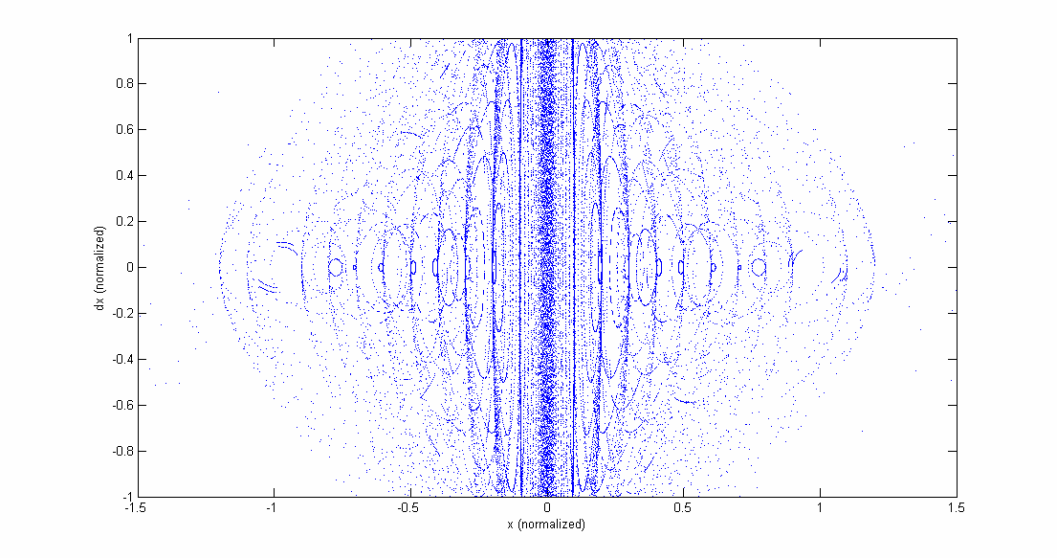

Figure 3. Poincaré map generated using ODE45.

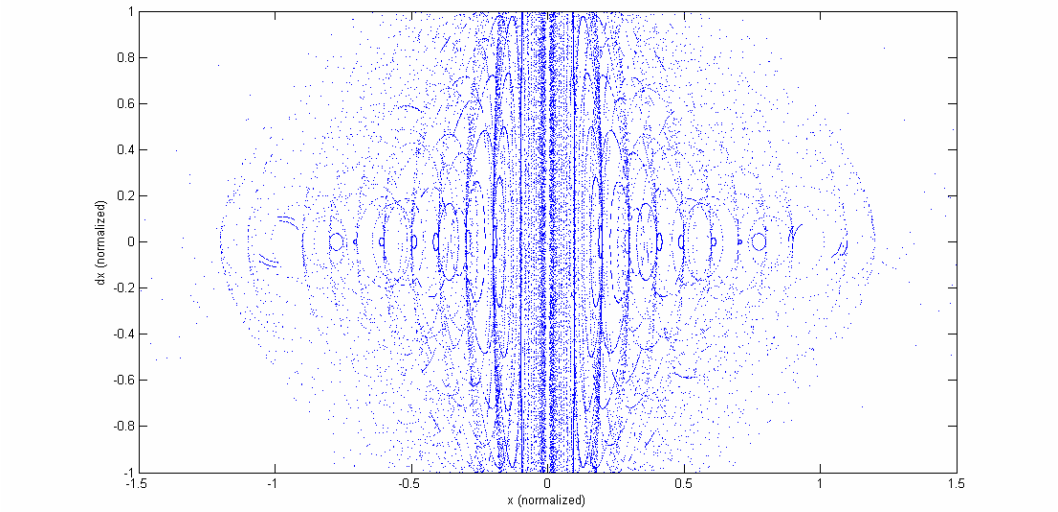

Figure 4. Poincaré map generated using the variational integrator.

Example 2: The General 4-Body Problem

In the following example we will derive a variational integrator for the general 4-body problem. We begin by deriving the Lagrangian for the general N-body problem, where the kinetic energy is given by

$$T = \frac{1}{2}\sum_{i=1}^{N} m_i\left(\dot{x}_i^2 + \dot{y}_i^2 + \dot{z}_i^2\right), \tag{28}$$

where m_i is the mass of the i-th body, and the potential energy is given by

$$V = -G\sum_{i=1}^{N-1}\sum_{j>i}^{N}\frac{m_i m_j}{r_{ij}}, \tag{29}$$

where G is the universal gravitational constant (6.6742E-11 $m^3kg^{-1}s^{-2}$) and $r_{ij} = \left|r_i - r_j\right|$. Thus, the Lagrangian is

$$L = \frac{1}{2}\sum_{i=1}^{N} m_i\left(\dot{x}_i^2 + \dot{y}_i^2 + \dot{z}_i^2\right) + G\sum_{i=1}^{N-1}\sum_{j>i}^{N}\frac{m_i m_j}{r_{ij}} \tag{30}$$

Explicitly for the 4-body problem, the Lagrangian is

$$L = \frac{1}{2}\sum_{i=1}^{4} m_i\left(\dot{x}_i^2 + \dot{y}_i^2 + \dot{z}_i^2\right) + G\left(\frac{m_1 m_2}{r_{12}} + \frac{m_1 m_3}{r_{13}} + \frac{m_1 m_4}{r_{14}} + \frac{m_2 m_3}{r_{23}} + \frac{m_2 m_4}{r_{24}} + \frac{m_3 m_4}{r_{34}}\right). \tag{31}$$

Since the Lagrangian is of the form of Eq. (2), then we can apply Eqs. (17a) and (17b) directly to solve for the position and momentum at the next time step. Recall Eq. (17),

$$q_{k+1} = q_k + (\Delta t)M^{-1}p_k - \frac{1}{2}(\Delta t)^2 M^{-1}\left(\nabla V(q_k)\right) \tag{17a}$$

$$p_{k+1} = p_k - \frac{1}{2}(\Delta t)\left(\nabla V(q_{k+1}) + \nabla V(q_k)\right) \tag{17b}$$

where the 12-by-1 vector $\nabla V(q_k) = \left[\partial V/\partial q_{1,k} \quad \partial V/\partial q_{2,k} \quad \partial V/\partial q_{3,k} \quad \partial V/\partial q_{4,k}\right]^T$, and

$$\frac{\partial V}{\partial q_{1,k}} = G\left[\frac{m_1 m_2(q_{1,k} - q_{2,k})}{r_{12}^3} + \frac{m_1 m_3(q_{1,k} - q_{3,k})}{r_{13}^3} + \frac{m_1 m_4(q_{1,k} - q_{4,k})}{r_{14}^3}\right]$$

$$\frac{\partial V}{\partial q_{2,k}} = G\left[-\frac{m_1 m_2(q_{1,k} - q_{2,k})}{r_{12}^3} + \frac{m_2 m_3(q_{2,k} - q_{3,k})}{r_{23}^3} + \frac{m_2 m_4(q_{2,k} - q_{4,k})}{r_{24}^3}\right]$$

$$\frac{\partial V}{\partial q_{3,k}} = G\left[-\frac{m_1 m_2(q_{1,k} - q_{2,k})}{r_{13}^3} - \frac{m_2 m_3(q_{2,k} - q_{3,k})}{r_{23}^3} + \frac{m_3 m_4(q_{3,k} - q_{4,k})}{r_{34}^3}\right]$$

$$\frac{\partial V}{\partial q_{3,k}} = G\left[-\frac{m_1 m_4(q_{1,k} - q_{4,k})}{r_{14}^3} - \frac{m_2 m_4(q_{2,k} - q_{4,k})}{r_{24}^3} - \frac{m_3 m_4(q_{3,k} - q_{4,k})}{r_{34}^3}\right]$$

for q equals to *x, y,* and *z*. Thus, given a set of initial conditions $\left\lfloor q_1, p_{q1}, q_2, p_{q2}, q_3, p_{q3}, q_4, p_{q4}\right\rfloor$ Eqs. (17) and (29) allows us to map the states from step k to k+1 explicitly.

As a numerical exercise we will look at the four body problem with the Sun, Jupiter, Saturn, and Uranus system, with their initial conditions specified in the J2000 frame with respect to the solar system barycenter on 01-JAN-2000 (Appendix B). Figure 5 is an example of a 10,000 years propagation of the system with integration step size of 5 days using RK4 scheme. The purpose of Figure 5 is for schematical references only.

In this example we will, again, compare the variational integrator with that of ODE45 and RK4 in Matlab. The trajectory propagated using ODE45 is considered our "true" trajectory. We begin by looking at the error in the total energy and the total linear momentum of the system for the 100 years. Figure 6 shows the error in the total energy for the three schemes, the variational integrator (VI) scheme derived above, RK4, and ODE45. A step size of 1 day was selected for the variational and RK4 integrators. Two tolerance settings were analyzed for ODE45, 1E-10 and 5E-14. The run times were:

scheme	runtime
VI	61.282 secs
RK4	222.594 sec
ODE45 (tol: 1.0E-10)	30.422 sec
ODE45 (tol: 5.0E-14)	32.734 sec

Note from Figure 6 that the total energy error for VI, RK4, and ODE45(tol: 5.0E-14) are fairly constant in its plotted scale (ODE45(tol: 5.0E-14) is right above the RK4 plot). We also see a clear energy drift for the ODE45 with tolerances set at 1.0E-10. Figure 7 is similar to Figure 6 but with the y-axis rescaled to show the variation in the errors for RK4 and ODE45(tol: 5.0E-14). Note again that the energy drift for ODE45 and the near constant behavior of RK4 for this system. Figure 8 shows the error in the total linear momentum of the 4-body system. Note the fairly constant behavior of the ODE45 scheme at either tolerance settings.

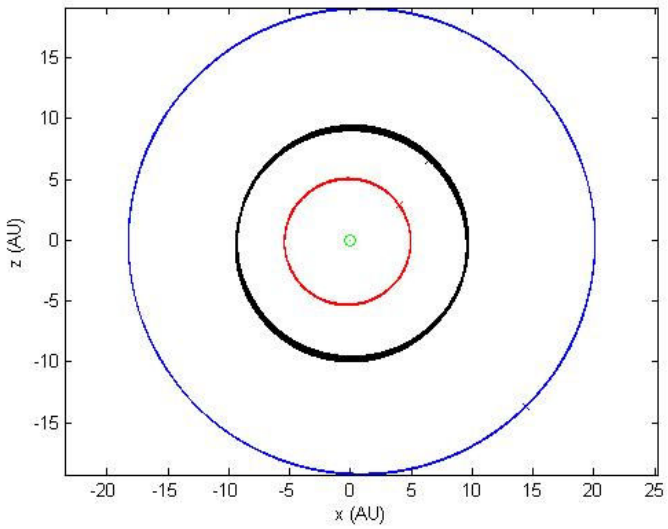

Figure 5. Propagation of the 4-body problem (Sun, Jupiter, Saturn, and Uranus) for 10,000 years with integration step size of 5 days using RK4.

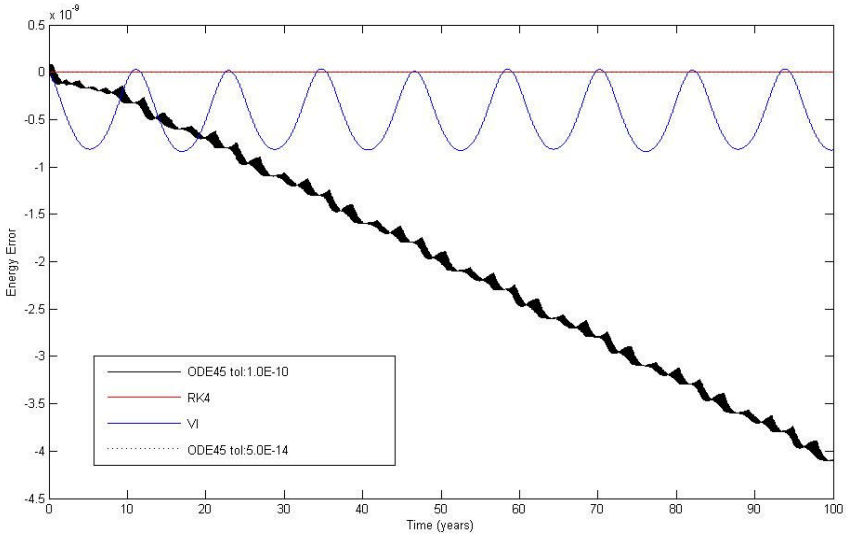

Figure 6. Energy error ($\Delta E/E_0$) for 100 year integration with 1 day step sizes for the variational integrator and the RK4.

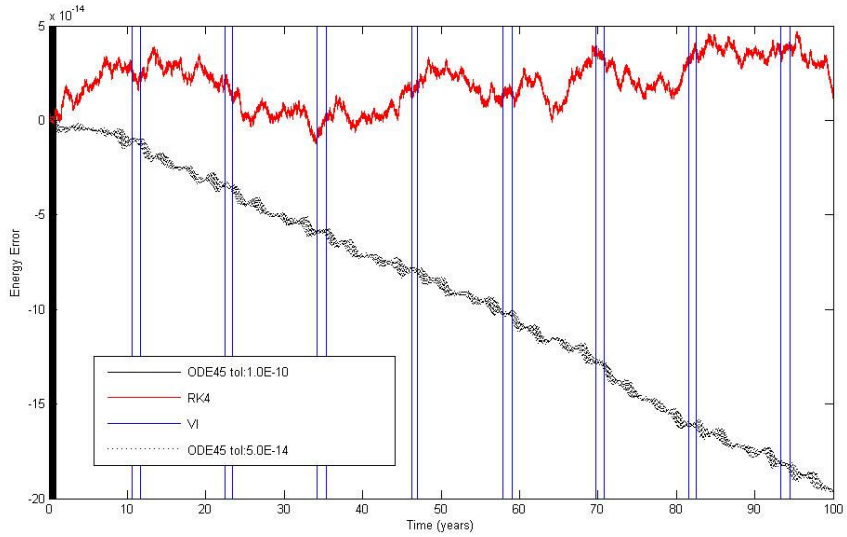

Figure 7. Rescaled view of Figure 6 to show the energy drift associated with the ODE45 with tolerance set at 5.0E-14. 100 year integration with 1 day step sizes for the variational integrator and the RK4.

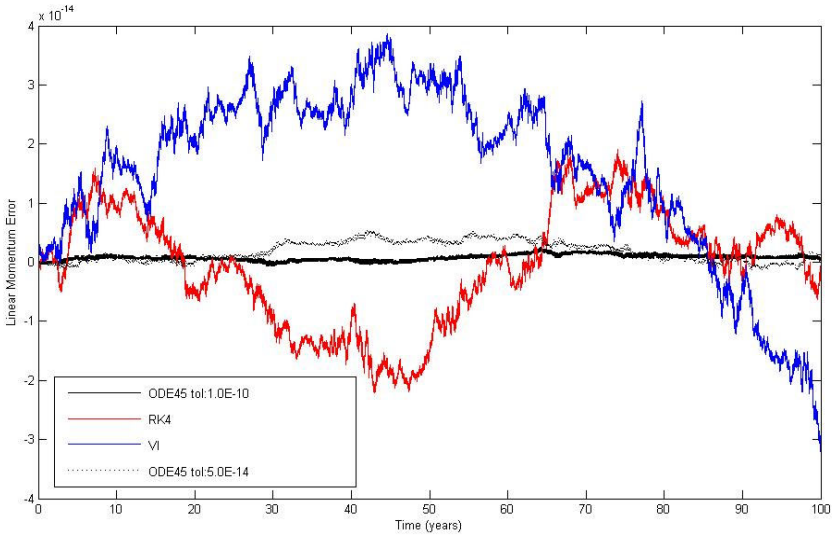

Figure 8. Total linear momentum error ($\Delta p/p_0$) for 100 year integration with 1 day step sizes for the variational integrator and the RK4.

The example above integrates the solution for a very short duration, and we noted that the ODE45 and RK4 schemes perform remarkably when well comparing energy and momentum errors. For ODE45 a distinct drift appears in Figure 6 and even in Figure 7 which has tolerances set to 5.0E-14, which is near machine precision for Matlab. Thus, by observation we will qualitatively state that this drift will continue to grow as we propagate for longer time periods. on The behavior of the RK4 scheme appears to be near constant for the 100 year propagation, but for the 100,000 years propagation (Figure 9b) we note that drifts in the energy do occur. As we decrease the integration step size the energy drift is slower, but the "signature" of the drift is apparent, which lead us to conclude that increases in integration time will lead to growth in the energy error. On the other hand Figure 9b shows the energy error for the variational integrator for various step sizes, and one note the constant average behavior of the energy for the range of step sizes.

From Figure 9 we note the wide range of acceptable step sizes for the variational integrator, because the integrator is developed using the Lagrangian of the system it inherently understands the structure of the dynamical system while arbitrary integrators such as RK4 and ODE45 does not. This symplectic nature of the variational integrator allows one to take much larger integration steps. As an example, Figure 10 shows the integration of the 4-body problem for 500,000 years with 200 day step sizes. This is not achievable using RK4. Note that even at this large time step the energy error remains with 0.45%.

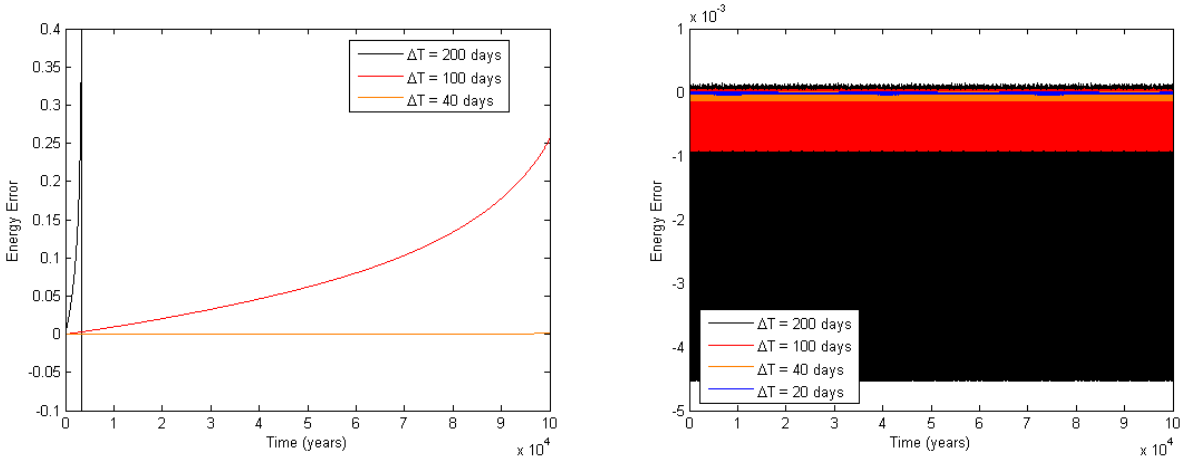

Figure 9. Energy error ($\Delta E/E_0$) for 100,000 year integration for various step sizes using (a) RK4 and (b) VI.

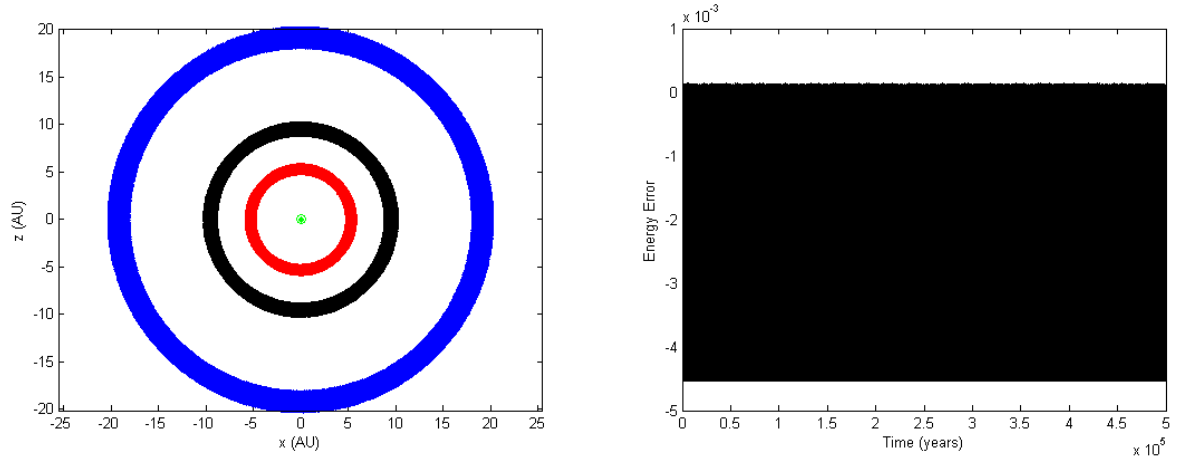

Figure 10. (a) Trajectory plot for Sun, Jupiter, Saturn and Uranus integrated for 500,000 years using a variational integrator with 200 day step sizes. (b) Energy error associated with (a).

Conclusion

Variational integrators are straight forward to design and implement for simple dynamical systems, the benefit of these integrators is that they inherently conserved important quantities of the mechanical system. Here we derived and implemented a variational integrator for the planar circular restricted three-body problem (PCR3BP) and the simplified 4-body solar system model, containing only the Sun, Jupiter, Saturn, and Uranus. A surprising conclusion is that RK4 perform very well (for small time steps) for many applications where short integration times are sufficient, i.e., many mission design and navigation. But for long-term propagations and for larger step sizes, variational integrators are very beneficial: no energy bias, faster integration time over the RK4, and reasonably accurate solutions for small integration steps.

Reference

1. A. Hirani, *Linearization Methods for Variational Integrators and Euler-Lagrange Equations*, Master Thesis, California Institute of Technology, 2000.

2. Z. Ge and J. E. Marsden, "Lie-Poisson Hamilton-Jacobi Theory and Lie-Poisson Integrators," *Physics Letters A*, volume 133, **3**, 134-139, 1988.

3. M. Ortiz, "A Note on Energy Conservation and Stability of Nonlinear Time-Stepping Algorithms," *Comput. Structures* **24**, 167-168, 1986.

4. J. M. Wendlandt and J. E. Marsden, "Mechanical Integrators Derived from a Discrete Variational Principle," *Physica D*, **106**, 223-246, 1997.

5. M. West, *Variational Integrators*, Ph.D. Thesis, California Institute of Technology, 2004.

6. J. E. Marsden and M. West, "Discrete Mechanics and Variational Integrators," *Acta Numerica* **10**, 357-514, 2001.

7. J. M. Sanz-Serna, "Symplectic integrators for Hamiltonian problems: An Overview," *Acta Numerica*, 243-286, 1992.

8. A. Lew, J. E. Marsden, M. Ortiz, and M. West, "An Overview of Variational Integrators," *Finite Element Methods: 1970's and Beyond*, L. P. Franca (Ed.), 2003.

9. A. Lew, J. E. Marsden, M. Ortiz, and M. West, "Variational Time Integrators," *Int. J. Numer. Meth. Engr*. **60**, 153-212, 2004.

10. J. E. Marsden and T. Ratiu, *Introduction to Mechanics and Symmetry*, vol. 17 of *Texts in Applied Mathematics*. Springer: Berlin, 2nd Edition, 1999.

11. H. Goldstein, C. Poole, and J. Safko, *Classical Mechanics*. Addison Wesley, 3rd Edition, 2002.

12. W. H. Press, S. A. Teukolsky, W. T. Vetterling and B. P. Flannery, *Numerical Recipes in C: The Art of Scientific Computing, 2nd ed*. Cambridge University Press, 1992.

Appendix A: Fourth Order Runge-Kutta

The problem in ordinary differential equations is reduced to the study of a set of N coupled first-order differential equations for the functions y_i, for i = 1, 2, …, N, having the general form $dy_i / dx = f_i(x, y_1, \ldots, y_N)$ and $\bar{y}(0) = \bar{y}_0$. For this system the Runge Kutta 4th order method is given by [12]

$$y_{i+1} = y_i + \frac{1}{6}(k_1 + 2k_2 + 2k_3 + k_4)h \tag{A.1}$$

where h is the time step and

$$k_1 = f(x_i, y_i)$$
$$k_2 = f\left(x_i + \frac{1}{2}h, y_i + \frac{1}{2}k_1 h\right)$$
$$k_3 = f\left(x_i + \frac{1}{2}h, y_i + \frac{1}{2}k_2 h\right)$$
$$k_4 = f(x_i + h, y_i + k_3 h)$$

The fourth-order Runge-Kutta method requires four evaluations of the right-hand side per step h. In general Runge-Kutta methods propagate a solution over an interval by combining the information from several Euler-style steps, which requires one evaluation of the right-hand side of the equation. This information is then used to match a Taylor series expansion up to some higher order, in this case the 4th order.

Appendix B: Sun, Jupiter, Saturn, and Uranus Initial Conditions (J2000)

```
% Symbol meaning [1 AU=149597870.691 km, 1 day=86400.0 s]:
%     JDCT     Epoch Julian Date, Coordinate Time
%       EC     Eccentricity, e
%       QR     Periapsis distance, q (AU)
%       IN     Inclination w.r.t xy-plane, i (degrees)
%       OM     Longitude of Ascending Node, OMEGA, (degrees)
%       W      Argument of Perifocus, w (degrees)
%       Tp     Time of periapsis (Julian day number)
%       N      Mean motion, n (degrees/day)
%       MA     Mean anomaly, M (degrees)
%       TA     True anomaly, nu (degrees)
%       A      Semi-major axis, a (AU)
%       AD     Apoapsis distance (AU)
%       PR     Orbital period (day)

% Sun Location wrt. solar system barycenter (J2000 at 1/1/2000):
EC= 2.695053498373502E-01;
QR= 5.099089718717647E-03;
IN= 1.554705636543432E+00;
OM= 1.036619948482233E+02;
W = 2.230251010937590E+02;
Tp=  2452714.788207898382;
N = 8.295806406050966E-02;
MA= 2.629151558798974E+02;
TA= 2.346698719568884E+02;
A = 6.980324520627633E-03;
AD= 8.861559322537618E-03;
PR= 4.339541961073438E+03;

% Jupiter Barycenter wrt. solar system barycenter (J2000 at 1/1/2000):
```

```
EC= 4.519473745552920E-02;
QR= 4.940999578022153E+00;
IN= 1.304247226688400E+00;
OM= 1.004854765769709E+02;
W = 2.728742185989755E+02;
Tp=  2451294.373235398438;
N = 8.376499808282183E-02;
MA= 2.095186795730955E+01;
TA= 2.290628657075529E+01;
A = 5.174876775244024E+00;
AD= 5.408753972465894E+00;
PR= 4.297737816982381E+03;

% Saturn Barycenter wrt. solar system barycenter (J2000 at 1/1/2000):
EC= 5.208961869783253E-02;
QR= 9.028846478354428E+00;
IN= 2.485923617209939E+00;
OM= 1.136522873810954E+02;
W = 3.396769407760255E+02;
Tp=  2452836.023406617343;
N = 3.354881072980565E-02;
MA= 3.166709256782745E+02;
TA= 3.123758885869840E+02;
A = 9.525000101751479E+00;
AD= 1.002115372514853E+01;
PR= 1.073063372944444E+04;

% Uranus Barycenter wrt. solar system barycenter (J2000 at 1/1/2000):
EC= 4.728166197021166E-02;
QR= 1.828060524979731E+01;
IN= 7.722234461097661E-01;
OM= 7.399981956645530E+01;
W = 9.694383222297407E+01;
Tp=  2439418.394472621381;
N = 1.173397107107506E-02;
MA= 1.422873714630614E+02;
TA= 1.454517356530984E+02;
A = 1.918783812601048E+01;
AD= 2.009507100222365E+01;
PR= 3.068015063437659E+04;
```